Laser Phys. Lett. **6**, No. 4, 282–289 (2009) / **DOI** 10.1002/lapl.200810136

Abstract: Laser performance of Yb:YAG ceramics and single-crystals doped with different Yb concentrations was investigated using two-pass pumping miniature laser configuration. Highly efficient laser performance was obtained for both Yb:YAG ceramics and single-crystals. For the low doping concentration, the laser performance of ceramics is lower than those of their single-crystal counterpart. However, better laser performance was observed for heavy-doped Yb:YAG ceramic than single-crystal ($C_{\mathrm{Yb}} = 20$ at.%). The maximum optical-to-optical efficiency decreases with Yb doping concentration for both Yb:YAG ceramics and crystals. However, the decrease of maximum optical-to-optical efficiency is faster for Yb:YAG crystals than that for Yb:YAG ceramics with Yb doping concentration. The effects of Yb concentration and the transmission of the output couplers on the laser performance and output laser wavelength of Yb:YAG ceramics and crystals were addressed by taking account into the intracavity laser intensity and reabsorption.

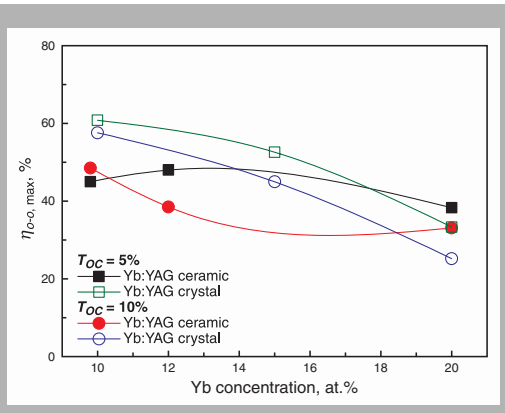

Comparison of the maximum optical-to-optical efficiency of Yb:YAG miniature lasers as a function of Yb concentration. The solid lines were used for illustration

Comparative study the effect of Yb concentrations on laser characteristics of Yb:YAG ceramics and crystals

J. Dong, [1,2,*] *K. Ueda,* [2] *H. Yagi,* [3] *A.A. Kaminskii,* [4] *and Z. Cai* [1]

[1] Institute of Optoelectronic Technology, Department of Electronic Engineering, Xiamen University, Xiamen 361005, China
[2] Institute for Laser Science, University of Electro-Communications, 1-5-1 Chofugaoka, Chofu, Tokyo 182-8585, Japan
[3] Konoshima Chemical Co., Ltd., 80 Kouda, Takuma, Mitoyo-gun, Kagawa 769-1103, Japan
[4] Institute of Crystallography, Russian Academy of Sciences, 59, Leninskii pr., Moscow 119333, Russia

Received: 5 December 2008, Revised: 12 December 2008, Accepted: 15 December 2008
Published online: 29 December 2008

Key words: Yb:YAG; ceramic; single-crystal; concentration-dependent laser properties

PACS: 42.55.Xi, 42.70.Hj, 42.60.Lh

1. Introduction

Ytterbium doped laser materials have been intensely investigated for developing high power laser-diode pumped solid-state lasers around 1 μm [1]. Yb:YAG as crystals and polycrystalline ceramics are one of the dominant laser gain medium used for solid-state lasers [2–6] owing to the excellent optical, thermal, chemical, and mechanical properties [7]. Owing to the small radius difference between yttrium ions and ytterbium ions [8], Yb:YAG single-crystal doped with different Yb concentrations can be grown by different crystal growth methods and efficient laser performance has been achieved [3,9,10]. By introducing Cr ions into Yb:AG crystal, self-Q-switched laser crystal was grown successfully and efficient laser operation was achieved in Cr,Yb:YAG self-Q-switched laser crystal pumped by laser-diode [11]. Multi-mode competition and spatial-hole burning effects induced switchable pulse generation was also observed in passively Q-switched Yb:YAG/Cr:YAG microchip lasers [12].

Transparent laser ceramics [6,13–16] fabricated by the vacuum sintering technique and nanocrystalline technology [17] have been proven to be potential replacements for counterpart single crystals because they have several

* Corresponding author: e-mail: jundong_99@yhaoo.com

remarkable advantages compared with single-crystal laser materials, such as high concentration and easy fabrication of large-size ceramics samples, multilayer and multifunctional ceramics laser materials [18,19]. Rare earths ions doped Lu_2O_3, Sc_2O_3, and Y_2O_3 oxides ceramics have been developed and their mechanical and optical properties are reported recently [20–23]. New nonlinear laser effects and Raman induced Stokes and anti-Stokes lasing effects were observed in these ceramics with excellent optical properties. The polarization properties of laser-diode pumped Nd:YAG ceramic was also investigated [24] and found that the linearly polarized laser can be achieved by adjusting the cavity symmetry even with random distribution of Nd:YAG gains in ceramic host. Passively Q-switched Yb:YAG/Cr:YAG all-ceramics microchip lasers have been reported with high peak power and sub-nanosecond pulse width [25–27]. Highly efficient laser operation was also obtained in these microchip passively Q-switched lasers. Efficient and high power laser operation in Nd^{3+}- and Yb^{3+}-ions doped YAG ceramics has been demonstrated [6,15]. Yb:YAG has been a promising candidate for high-power laser diode pumped solid-state lasers with rod [28], slab [29], and thin disk [30,31] configurations. The quasi-three-level laser system of Yb:YAG requires high pumping intensity to overcome transparency threshold and achieve efficient laser operation at room temperature [32]. The thin disk laser has been demonstrated to be a good way to generate high power with good beam quality owing to the efficiently cooling of gain medium and good overlap of the pump beam and laser beam [30]. However, in the thin disk case, the pump beam must be folded many times into thin laser gain medium disk with mirrors in order to absorb sufficient pump power, which makes the laser system extremely complicated. Some applications require that the lasers should be compact and economic; therefore, the cooling system is eliminated in compact and easily maintainable laser system. Therefore, laser-diode end-pumped microchip lasers are a better choice to achieve highly efficient laser operation under high pump power intensity. The thinner the gain medium, the better the cooling effect, therefore, heavy doped Yb:YAG gain media are the better choice for such lasers. The development of Yb:YAG ceramics doped with 1 at.% Yb^{3+} ions have been reported [16], but the efficiency of such Yb:YAG ceramic laser is low owing to the deficient activator concentration. In principle, there is no concentration quenching effect in Yb:YAG, however, the unwanted impurities (such as Er^{3+}, Tm^{3+}, Ho^{3+}, and so on) from raw materials will be deleterious to the laser performance owing to the high activator doping. Concentration dependent optical properties and laser performance of Yb:YAG crystals have been reported [33–36]. The concentration quenching of Yb:YAG crystals has been investigated and it was found that fluorescence lifetime decreases when the Yb concentration is greater than 15 at.% and lifetime decreases up to 15% when the Yb concentration reaches to 25 at.% [34,37]. The fluorescence lifetime of Yb^{3+} doped materials is usually affected by the radiative trapping and concentration quenching effects [38]. Radiative trapping and concentration quenching effects become stronger with Yb concentration and there is a concentration region (from 15 to 25 at.% for Yb:YAG crystal), two trends compete each other and consequently compensate each other, leading to a constant value of measured fluorescence lifetime. Therefore special technologies have been taken to eliminate the radiative trapping effect when the fluorescence lifetime is measured for Yb doped materials. Optical-thin samples or powder sandwiched between two undoped YAG crystals were used to measure the radiative lifetime of Yb:YAG crystals [10,37]. The radiative lifetime of Yb:YAG crystal was found to decrease with Yb concentration. Optical spectra of Yb:YAG ceramics doped with different Yb^{3+}-lasant concentration (C_{Yb} = 9.8, 12, and 20 at.%) and efficient 9.8 at.% Yb:YAG ceramic microchip lasers [6] have been reported recently. The comparison of laser performance of Yb:YAG ceramic and single-crystal doped with 20 at.% Yb has been reported [39]. However, there is no systematic comparison studies of microchip laser performance of Yb:YAG ceramics and single-crystal doped with different Yb concentrations.

Here, we report on the systematical comparison of the performance of miniature Yb:YAG (C_{Yb} = 9.8, 12, and 20 at.%) ceramic and Yb:YAG single-crystals (C_{Yb} = 10, 15, and 20 at.%) lasers at 1030 nm with two-pass pumping scheme. The laser performance of Yb:YAG ceramics is nearly comparable to or better than their counterpart single crystals depending on the Yb doping concentration. The effect of Yb concentration on the optical-to-optical efficiency and laser emitting spectra was also addressed.

2. Experimental setup

To compare the laser performance of Yb:YAG ceramics and single-crystals, double-pass pumped miniature lasers were used in the experiments. To absorb sufficient pump power, high doping concentration was needed for thin gain medium. Therefore, high doping concentration Yb:YAG single-crystals and ceramics were used in the laser experiments. Three Yb:YAG ceramics samples (C_{Yb} = 9.8, 12, and 20 at.%) were used in the laser experiments. Comparable Yb:YAG single-crystals (C_{Yb} = 10, 15, and 20 at.%) were used to compare the laser characteristics with those of Yb:YAG ceramics. The size of the samples is 10 mm in diameter and 1 mm in thickness. Fig. 1 shows a schematic diagram of the experimental setup for laser-diode pumped Yb:YAG miniature laser. One surface of the sample was coated for antireflection both at 940 nm and 1.03 μm. The other surface was coated for total reflection at both 940 nm and 1.03 μm, acting as one cavity mirror and reflecting the pump power for increasing the absorption of the pump power. Plane-parallel fused silica output couplers with transmission (T_{oc}) of 5 and 10% were mechanically attached to the gain medium tightly. A 35-W high-power fiber-coupled 940 nm laser diode (Apollo, F35-940-

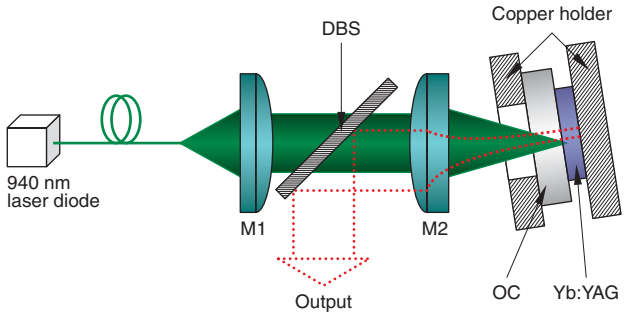

Figure 1 (online color at www.lphys.org) Schematic diagram of laser-diode pumped Yb:YAG ceramics and single-crystals miniature lasers. DBS – dichroic beam splitter; OC – output coupler; M1 – focus lenses with focal length of 8 mm; M2 – focus lenses with focal length of 15 mm

1) with a core diameter of 100 μm and numerical aperture of 0.22 was used as the pump source. Optical coupling system with two lenses M1 (8-mm focal length) and M2 (15-mm focal length) was used to focus the pump beam on the ceramic rear surface and to produce a pump light footprint on the Yb:YAG of about 170 μm in diameter. The laser spectrum was analyzed by using an optical spectrum analyzer (ANDO AQ6137) with resolution of 0.01 nm. Output beam profile of these lasers was monitored by using a CCD camera, and beam quality factor, M^2, was determined by measuring the beam diameters at different positions along the laser propagation direction.

3. Results and discussion

Fig. 2 shows the output power of miniature Yb:YAG ceramics and single-crystal lasers as a function of the absorbed pump power for different Yb concentrations and T_{oc}. The absorbed pump power for reaching laser thresholds of Yb:YAG ceramics (C_{Yb} = 9.8, 12, and 20 at.%) were 0.3, 0.33, and 0.64 W for T_{oc} = 5% and 0.33, 0.5, 0.68 W for T_{oc} = 10%. The pump power threshold increases with T_{oc} and Yb concentration for Yb:YAG ceramic lasers. This was caused by the increase of the losses introduced by the large T_{oc} and the increasing reabsorption of Yb^{3+} at lasing wavelength with Yb concentrations. For Yb:YAG ceramics doped with different Yb concentrations, the output power increases linearly with absorbed pump power for T_{oc} = 5 and 10%. The slope efficiencies respected to the absorbed pump power for Yb:YAG ceramics (C_{Yb} = 9.8, 12, and 20 at.%) were measured to be 50, 55, and 45% for T_{oc} = 5% and 52, 44, and 38% for T_{oc} = 10%. Slope efficiency increases with T_{oc} for 9.8 at.% Yb:YAG ceramic, however, the slope efficiencies decrease with T_{oc} for Yb:YAG ceramics doped with 12 and 20 at.% Yb^{3+} ions. Maximum output power of 2.54 W was measured for T_{oc} = 5% by using 12 at.% Yb:YAG ceramic as

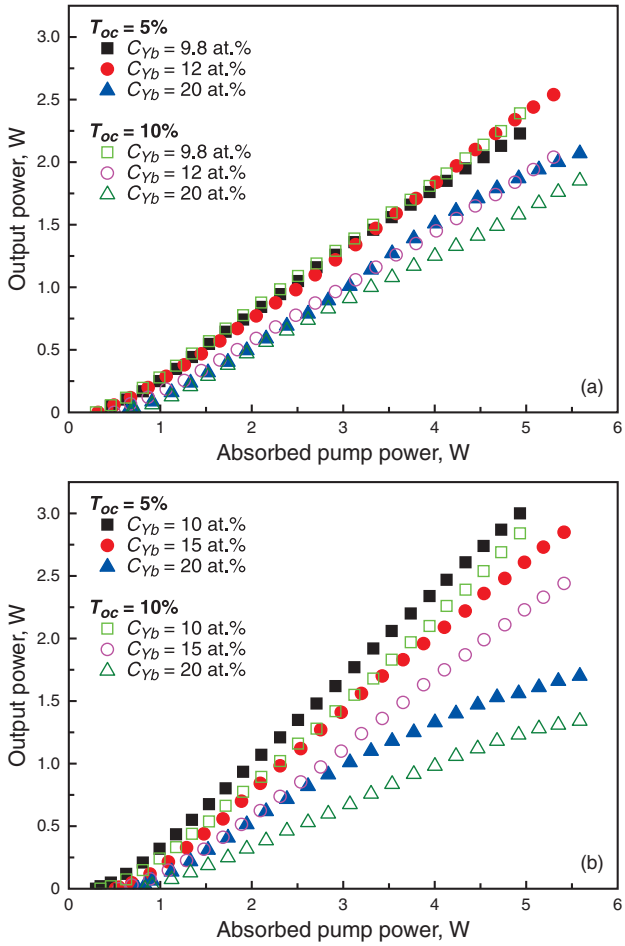

Figure 2 (online color at www.lphys.org) Output power of (a) Yb:YAG ceramic and (b) Yb:YAG single crystal miniature lasers as a function of absorbed pump power for different Yb concentrations and transmissions of the output couplings

gain medium when the absorbed pump power was 5.3 W. The corresponding optical-to-optical efficiency was about 48%.

The absorbed pump power for reaching laser thresholds of Yb:YAG single-crystal (C_{Yb} = 10, 15, and 20 at.%) were 0.3, 0.51, and 0.76 W for T_{oc} = 5% and 0.35, 0.55, and 0.84 W for T_{oc} = 10%. The absorbed pump power threshold increases with the T_{oc} and Yb concentrations, the same tendency as that for Yb:YAG ceramics. However, the absorbed pump power thresholds of Yb:YAG single crystals were higher than those of Yb:YAG ceramics. This may be caused by the pump configuration used in the laser experiments and low pump power intensity with pump beam diameter of 170 μm. Because the incident pump beam from laser-diode is several degrees away from the normal direction of the laser beam, there is a mismatch between the pump beam and laser beam. From Fig. 2b, we can see at low pump power just above absorbed

pump power threshold, the laser performance is lower than that high pump power levels, this is normal for the quasi-three-level system; efficient laser performance can be achieved at high pump power density [32]. However, for Yb:YAG ceramics, owing to the random distribution of Yb:YAG crystalline particles, the absorbed pump power threshold can be achieved more easily. Output power increases linearly with absorbed pump power for Yb:YAG single-crystals doped with 10 and 15 at.% Yb. The slope efficiencies of miniature lasers based on Yb:YAG single-crystals doped with 10 and 15 at.% Yb were measured to be 69, 62% for $T_{oc}=5\%$ and 67, 55% for $T_{oc}=10\%$. The slope efficiencies of Yb:YAG crystals doped with 10 and 15 at.% Yb^{3+} were higher than those for Yb:YAG ceramics although the pump power thresholds were higher than those of Yb:YAG ceramics. At higher pump power density, the inversion population excited by the pump beam is well-over the threshold, and the modes matched very well, therefore, the laser oscillates at high slope efficiency, especially for Yb:YAG crystal doped with 10 and 15 at.% Yb. The better laser performance of these crystals compared to their counterpart ceramic suggests that the intracavity loss for Yb:YAG crystal lower than that of Yb:YAG ceramics.

For Yb:YAG single-crystal doped with 20 at.% Yb, the output power increases with the absorbed pump power, and tends to increase slowly when the absorbed pump power is higher than a certain value (e.g. 3 W for $T_{oc}=5\%$ and 2.3 W for $T_{oc}=10\%$), as shown in Fig. 2b. However, besides the higher absorbed pump power threshold compared to its counterpart Yb:YAG ceramic, the slope efficiencies (45% for $T_{oc}=5\%$ and 32 at.% for $T_{oc}=10\%$) of 20 at.% Yb:YAG single crystal were lower than those (47% for $T_{oc}=5\%$ and 38 at.% for $T_{oc}=10\%$) for its counterpart Yb:YAG ceramic. The laser results show that heavy doped Yb:YAG ceramic is better than its single crystal counterpart. The strong segregation of the impurities in Yb:YAG crystal with increase of the Yb concentration during crystal growth is the main reason for the worse laser performance. The other reasons for the less efficient laser operation may be the impurities increases with doping concentration [33], the impurities induced concentration quenching effect limit the laser performance of highly doped Yb:YAG crystals. The green emission was observed in the Yb:YAG crystals and ceramics when they were pumped with laser diodes, and visible intensity increases with Yb concentration up to 15 at.% and then decreases with Yb concentration [40]. Energy transfer from Yb^{3+} ions to Er^{3+}, and Tm^{3+} impurities and cooperative energy transfer between Yb^{3+} ions are the causes of these visible luminescence. These are deleterious to the infrared laser operation. However, the distance between Yb^{3+} ions and impurities or other quenching centers is decreased with Yb concentration, the cooperative luminescence intensity decreases because the excited ions are more easily quenched by reaching a neighboring defect site. Therefore, the effect of cooperative energy transfer is not a main factor to limit the laser performance of highly doped Yb:YAG crystals. Fig. 3 shows the optical-to-optical efficiencies of Yb:YAG lasers as a function of absorbed pump power. Under present laser experimental conditions, there is no saturation effect of Yb:YAG lasers with different output couplings for Yb concentration equal to or less than 15 at.% although the optical efficiency increases slowly with the absorbed pump power. However, for 20 at.% Yb:YAG, there is saturation effect for ceramic lasers with $T_{oc}=5\%$ and for single-crystal lasers with different output couplings. Maximum optical efficiency of 48% was achieved for Yb:YAG ceramic doped with 12 at.% Yb at the absorbed pump power of 5.3 W. For single crystal doped with 20 at.% Yb lasants, there is a maximum optical efficiency for all output couplings (as shown in Fig. 3b). The optical-to-optical efficiency decreases with further increase of the pump power. For Yb:YAG ceramics, except the comparable laser performance of 9.8 at.% Yb:YAG with $T_{oc}=5$ and 10%, the optical-to-optical efficiency decreases with T_{oc} and Yb concentration. How-

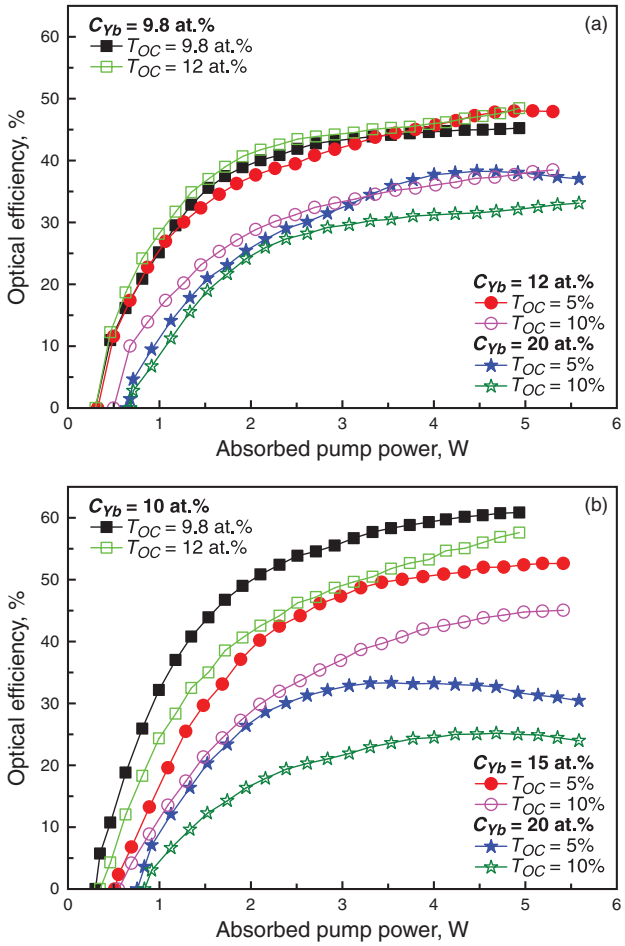

Figure 3 (online color at www.lphys.org) Optical efficiencies of (a) Yb:YAG ceramic and (b) Yb:YAG single crystal miniature laser as a function of absorbed pump power for different Yb concentrations and transmissions of the output coupler

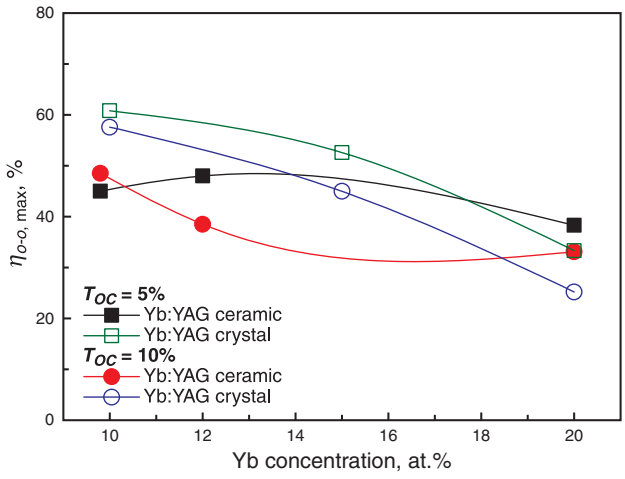

Figure 4 (online color at www.lphys.org) Comparison of the maximum optical-to-optical efficiency of Yb:YAG miniature lasers as a function of Yb concentration. The solid lines were used for illustration

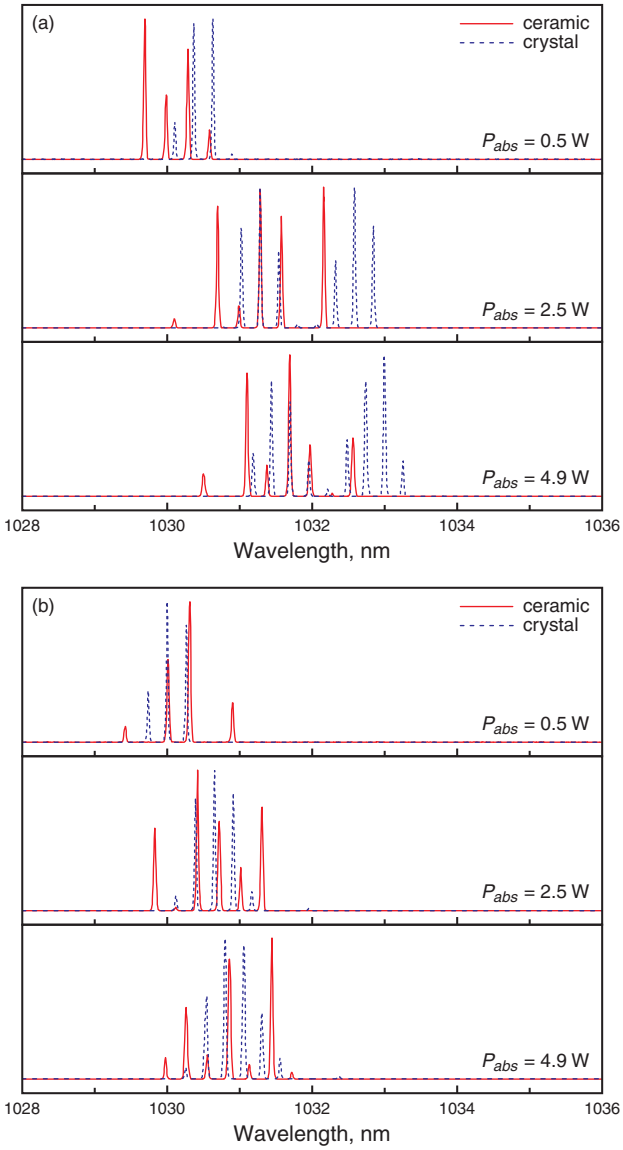

Figure 5 (online color at www.lphys.org) Laser emitting spectra of 9.8 at.% Yb:YAG ceramic and 10 at.% Yb:YAG crystal miniature lasers under different pump power levels; (a) – T_{oc} = 5%, (b) – T_{oc} = 10%. The resolution of the optical spectral analyzer is 0.01 nm

ever, for Yb:YAG single-crystals, the optical-to-optical efficiency decreases with the T_{oc} and Yb concentration under different pump power levels. Optical-tooptical efficiency of Yb:YAG crystal doped with less than 15 at.% Yb is higher than that forYb:YAG ceramics under certain pump power levels. For 20 at.% Yb:YAG, Yb:YAG ceramic has higher optical-to-optical efficiency than that of crystal under different pump power levels. The decrease of the optical-to-optical efficiency of Yb:YAG lasers with Yb concentration was attributed to the thick samples used for highly doped Yb:YAG samples. The better laser performance can be further improved through optimizing the thicknesses for Yb:YAG samples with different Yb concentrations. The highly efficient microchip lasers has been demonstrated by using the same crystals [36] as those here used.

Fig. 4 shows the maximum optical-to-optical efficiency under available pump power of Yb:YAG ceramics and single-crystals lasers as a function of Yb concentrations for different output couplings. For Yb:YAG single crystals, the maximum optical-to-optical efficiency decreases with Yb concentrations, there are 45% and 56% dropping for T_{oc} = 5 and 10% when Yb concentration increases from 10 to 20 at.%. However, for Yb:YAG ceramics, the maximum optical-to-optical efficiency decreases with Yb concentration, the decrease is smaller for Yb:YAG ceramics compared to that for Yb:YAG single crystal. There are 15 and 32% dropping for T_{oc} = 5 and 10% when Yb concentration increases from 10 to 20 at.% for Yb:YAG ceramics. Because small different optical properties were observed in Yb:YAG ceramics and single-crystals doped with different Yb concentrations[6,41], the different laser performance of Yb:YAG ceramics and single-crystals may be caused by the Yb^{3+}-ions distribution in YAG host and optical quality of Yb:YAG samples. Although the distribution coefficient of Yb in Yb:YAG is close to unit, there is still concentration gradient observed in Yb:YAG single crystals along the growth axis and radius of the crystal boule [42]. The Yb^{3+}-ion distribution inhomogeneity in Yb:YAG single-crystal becomes server with Yb concentration. The impurities such as Ho^{3+}, Er^{3+} increase with Yb concentration in Yb:YAG crystals because the strong segregation of rare-earth ions in YAG crystal was observed. This was observed in the reduced radiative lifetime in highly doped Yb:YAG crystals [10,33,37]. This

concentration quenching effect limits the efficient laser performance of highly doped Yb:YAG crystals. For ceramics, the distribution of Yb ions in the grains and grain boundary is a main factor to determine the optical properties. The gain boundary of YAG ceramics was measured to be less than 0.5 nm [43], and sintering temperature is about 200°C lower than the melt point of Yb:YAG crystal, the segregation of Yb in grain boundary can only be achieved by diffusion or migration, therefore the distribution of Yb in gain and boundary should be close to homogeneous. When Yb ions were doped in YAG ceramics, the segregation of ytterbium ions in the grain boundary, accompanied by a reduction of the acoustic mismatch, leads to increased phonon transmission [44]. This will be further enhanced by introducing more ytterbium ions. This may be one of the main reasons for the better laser performance of heavy doped Yb:YAG ceramics compared to that of single-crystal with same doping levels.

Fig. 5 shows the comparison of the laser emitting spectra of 9.8 at.% Yb:YAG ceramic and 10 at.% Yb:YAG single-crystal miniature lasers under different absorbed pump power for $T_{oc} = 5$, and 10%. Lasers operated at multi-longitudinal modes under different pump levels. The number of longitudinal modes increases with the absorbed pump power because the inversion population provided with pump power can overcome the threshold for low gain away from the highest emission peak of Yb:YAG gain medium. The longitudinal mode oscillation for these miniature Yb:YAG lasers was mainly caused by the etalon effect of plane-parallel Yb:YAG thin plate. The separation of longitudinal modes was measured to be 0.29 nm, which is in good agreement with the free spectral range (0.292 nm) of 1-mm-long cavity filled with gain medium predicted by [45] $\Delta\lambda_c = \lambda^2/2L_c$, where L_c is the optical length of the resonator and λ is the laser wavelength. And the center wavelength of the lasers shifts to longer wavelength with the pump power which is caused by the temperature dependent emission spectra of Yb:YAG crystal [41].

For $T_{oc} = 5\%$, both Yb:YAG ceramic and crystal lasers are oscillating at longer wavelength comparing to those for $T_{oc} = 10\%$. The cause of the wavelength shift to longer wavelength for $T_{oc} = 5\%$ is relating to the change of the intracavity laser intensity [46] because only the intracavity laser intensity is different for both cases. Intracavity laser intensity for $T_{oc} = 5\%$ is about two times higher than that for $T_{oc} = 10\%$, therefore, more longitudinal modes will also be excited for $T_{oc} = 5\%$. Because the better laser performance for 10 at.% Yb:YAG lasers compared to 9.8 at.% Yb:YAG ceramics lasers, the intracavity intensity is higher for crystal laser, therefore Yb:YAG crystal lasers oscillate at longer wavelength than those for Yb:YAG ceramics lasers, especially for $T_{oc} = 5\%$. Strong mode competition and mode hopping in these Yb:YAG ceramic lasers were also observed. When the laser oscillates, the excited Yb^{3+} ions jump back to the lower laser level, they always relax to other even-lower energy levels or ground level, this process is rapid compare to the lifetime of Yb^{3+} ion in YAG crystal or ceramics. The relaxation of Yb^{3+} ions to the lower energy or ground levels causes the lower-level population to increase with the lasing intensity, this increases the reabsorption. This enhanced reabsorption provide a negative feedback process for the lasing modes and effective gain profile of Yb:YAG medium. This negative feedback process accompanied with the effects of strong mode competition makes some stronger laser modes eventually faded or quenched. When the intracavity light intensity is high enough, the population distribution at lower energy levels is changed dramatically. At the same time,

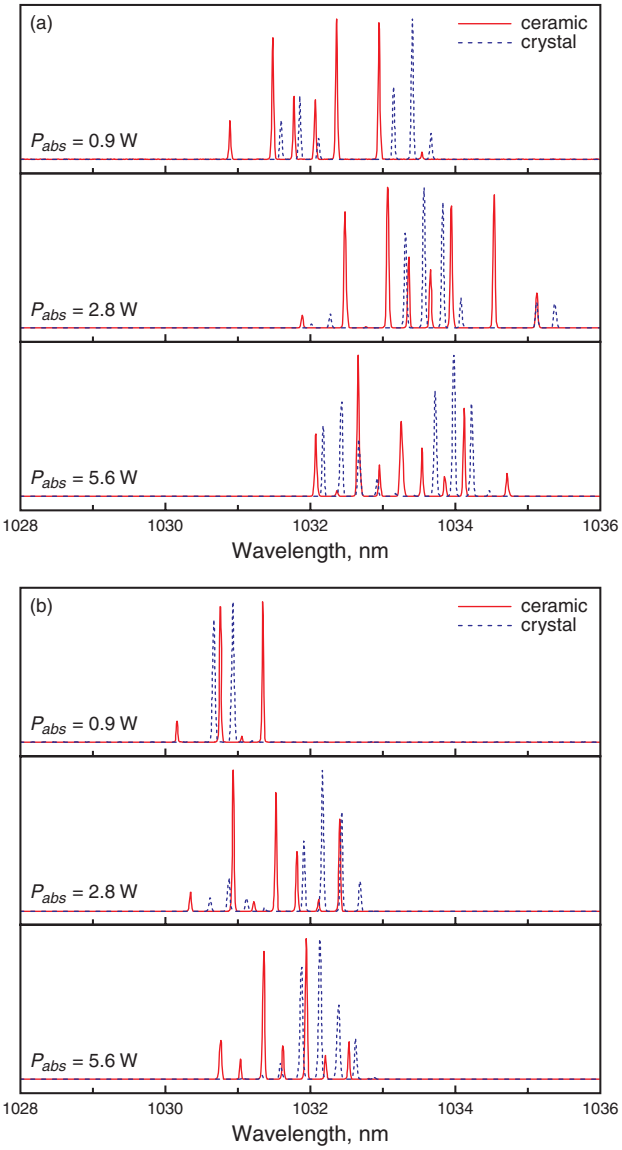

Figure 6 (online color at www.lphys.org) Laser emitting spectra of 20 at.% Yb:YAG ceramic and crystal miniature lasers under different pump power levels; (a) – $T_{oc} = 5\%$, (b) – $T_{oc} = 10\%$. The resolution of the optical spectral analyzer is 0.01 nm

the effective gain curve of Yb:YAG under lasing condition was altered by the strong reabsorption and temperature rise induced by the absorption pump power. Some initially suppressed modes at longer wavelength governed by the emission spectra can oscillate under changed gain curve, therefore the laser wavelength shifts to longer wavelength and mode hopping was observed. Fig. 6 shows the laser emitting spectra of 20 at% Yb:YAG ceramic and single-crystal miniature lasers under different pump power levels and output couplings. The lasers oscillate at multi-longitudinal modes. The number of the longitudinal modes increases with the pump power. The laser oscillates at longer wavelength for 20 at.% Yb:YAG lasers compared to that for 10 at.% Yb:YAG lasers for both transmissions of the output couplers (as shown in Fig. 5 and Fig. 6). The red-shift of laser wavelength for $T_{oc} = 10\%$ with Yb concentration is smaller than that for $T_{oc} = 5\%$ because of the lower intracavity laser intensity Yb:YAG lasers with $T_{oc} = 10\%$. The number of longitudinal modes is larger for $T_{oc} = 5\%$ than that for $T_{oc} = 10\%$. This may be related to the gain curve change due to the strong reabsorption under strong intracavity intensity.

The output beam transverse intensity profiles were also monitored in all the pump power range. One example of the beam intensity profile at output power of 2.5 W for 12 at.% Yb:YAG ceramics with $T_{oc} = 5\%$ was shown in Fig. 7, as well as a horizontal slice through the center. The output beam profile is close to TEM_{00} mode. The measured spatial profile can be fitted with Gaussian function very well, as shown in Fig. 7b. Near-diffraction-limited beam quality with M^2 of less than 1.1 was achieved in these miniature lasers with Yb:YAG ceramics and single-crystals as gain media in the available pump power range.

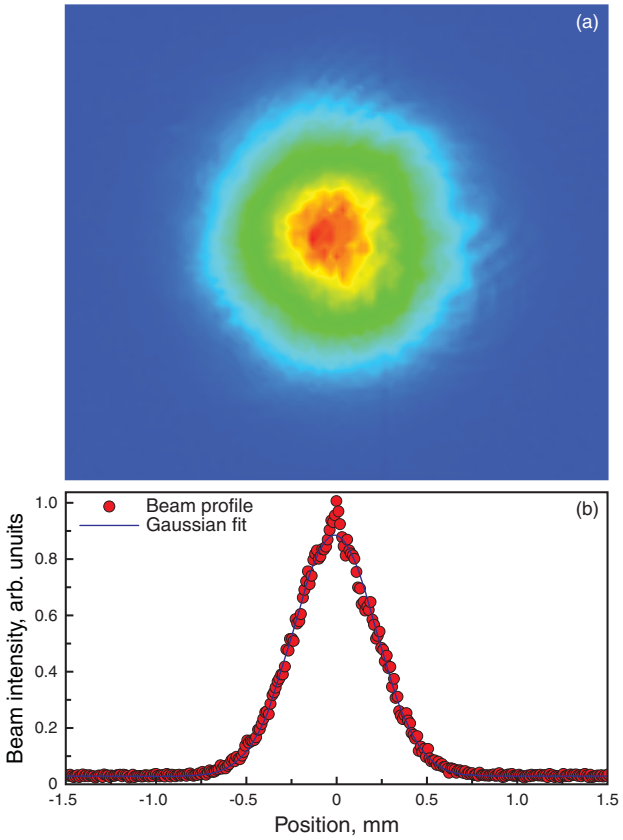

Figure 7 (online color at www.lphys.org) (a) – output laser beam profile of Yb:YAG ceramic miniature lasers when output power is 2.5 W for 12 at.% Yb:YAG ceramics with $T_{oc} = 5\%$; (b) – horizontal slice through center of beam profile with Gaussian fit

4. Conclusions

In conclusion, systematic comparison of laser performance was done for Yb:YAG ceramics and single-crystals doped with different concentrations. Although the pump power thresholds of Yb:YAG crystals were higher than their ceramics counterparts due to the pump configuration, the efficient laser operation was obtained by using both Yb:YAG ceramics and single-crystals. The laser performance of 1-mm-thick Yb:YAG ceramics and crystals becomes worse with Yb concentration under present miniature laser configuration. However, the laser performance of Yb:YAG crystals is more sensitive to the Yb concentrations, while the laser performance of Yb:YAG ceramics is less sensitive to the Yb concentrations. The laser performance of low doping Yb:YAG ceramics is worse than those obtaining from Yb:YAG singly crystals. The laser performance of 20 at.% Yb:YAG ceramics is better than its counterpart single crystal. Both Yb:YAG ceramics and crystals miniature lasers oscillate at multi-longitudinal modes, the number of longitudinal-mode increases with absorbed pump power. Strong mode competition and mode hopping were observed in these Yb:YAG lasers. The strong reabsorption and gain curve change under high intracavity laser intensity play important roles on the red-shift of the output laser wavelength. High beam quality lasers with M^2 less than 1.1 were achieved by adopting Yb:YAG ceramics and crystals as gain media. Heavy-doped Yb:YAG ceramic will be a potential candidate for microchip lasers by optimizing the thickness and Yb^{3+} concentration.

Acknowledgements This work was supported by the 21st Century Center of Excellence (COE) program of Ministry of Education, Science, Sports and Culture of Japan, and by the Russian Foundation for Basic Research, as well as by the Program "Femtosecond physics and new optical materials" of Presidium of Russian Academy of Sciences.

References

[1] W.F. Krupke, IEEE J. Sel. Top. Quantum Electron. **6**, 1287 (2000).

[2] P. Lacovara, H.K. Choi, C.A. Wang, R.L. Aggarwal, and T.Y. Fan, Opt. Lett. **16**, 1089 (1991).
[3] U. Brauch, A. Giesen, M. Karszewski, Chr. Stewen, and A. Voss, Opt. Lett. **20**, 713 (1995).
[4] T. Taira, J. Saikawa, T. Kobayashi, and R.L. Byer, IEEE J. Sel. Top. Quantum Electron. **3**, 100 (1997).
[5] H.W. Bruesselbach, D.S. Sumida, R.A. Reeder, and R.W. Byren, IEEE J. Sel. Top. Quantum Electron. **3**, 105 (1997).
[6] J. Dong, A. Shirakawa, K. Ueda, H. Yagi, T. Yanagitani, and A.A. Kaminskii, Appl. Phys. Lett. **89**, 091114 (2006).
[7] G.A. Bogomolova, D.N. Vylegzhanin, and A.A. Kaminskii, Zh. Exp. Teor. Fiz. **42**, 440 (1976).
[8] Ł. Dobrzycki, E. Bulska, D.A. Pawlak, Z. Frukacz, and K. Woźniak, Inorg. Chem. **43**, 7656 (2004).
[9] J. Dong, A. Shirakawa, K. Ueda, J. Xu, and P. Deng, Appl. Phys. Lett. **88**, 161115 (2006).
[10] F.D. Patel, E.C. Honea, J. Speth, S.A. Payne, R. Hutcheson, and R. Equall, IEEE J. Quantum Electron. **37**, 135 (2001).
[11] J. Dong, A. Shirakawa, S. Huang, Y. Feng, K. Takaichi, M. Musha, K. Ueda, and A.A. Kaminskii, Laser Phys. Lett. **2**, 387 (2005).
[12] J. Dong, A. Shirakawa, and K. Ueda, Laser Phys. Lett. **4**, 109 (2007).
[13] J. Lu, M. Prabhu, J. Song, C. Li, J. Xu, K. Ueda, A.A. Kaminskii, H. Yagi, and T. Yanagitani, Appl. Phys. B **71**, 469 (2000).
[14] J. Lu, M. Prabhu, J. Song, C. Li, J. Xu, K. Ueda, H. Yagi, T. Yanagitani, and A.A. Kaminskii, Jpn. J. Appl. Phys. **40**, L552 (2001).
[15] J. Lu, K. Ueda, H. Yagi, T. Yanagitani, Y. Akiyama, and A.A. Kaminskii, J. Alloys Compd. **341**, 220 (2002).
[16] K. Takaichi, H. Yagi, J. Lu, A. Shirakawa, K. Ueda, T. Yanagitani, and A.A. Kaminskii, Phys. Status Solidi (a) **200**, R5 (2003).
[17] T. Yanagitani, H. Yagi, and Y. Hiro, Japan Patent No. 10-101411 (April 21, 1998).
[18] H. Yagi, T. Yanagitani, H. Yoshida, M. Nakatsuka, and K. Ueda, Jpn. J. Appl. Phys. **45**, 133 (2006).
[19] J. Dong, K. Ueda, A. Shirakawa, H. Yagi, T. Yanagitani, and A.A. Kaminskii, Opt. Express **15**, 14516 (2007).
[20] A.A. Kaminskii, M.Sh. Akchurin, P. Becker, K. Ueda, L. Bohatý, A. Shirakawa, M. Tokurakawa, K. Takaichi, H. Yagi, J. Dong, and T. Yanagitani, Laser Phys. Lett. **5**, 300 (2008).
[21] A.A. Kaminskii, H. Rhee, H.J. Eichler, K. Ueda, K. Takaichi, A. Shirakawa, M. Tokurakawa, J. Dong, H. Yagi, and T. Yanagitani, Laser Phys. Lett. **5**, 109 (2008).
[22] A.A. Kaminskii, N. Tanaka, H.J. Eichler, H. Rhee, K. Ueda, K. Takaichi, A. Shirakawa, M. Tokurakawa, Y. Kintaka, S. Kuretake, and Y. Sakabe, Laser Phys. Lett. **4**, 819 (2007).
[23] K. Takaichi, H. Yagi, P. Becker, A. Shirakawa, K. Ueda, L. Bohatý, T. Yanagitani, and A.A. Kaminskii, Laser Phys. Lett. **4**, 507 (2007).
[24] K. Otsuka and T. Ohtomo, Laser Phys. Lett. **5**, 659 (2008).
[25] J. Dong, A. Shirakawa, K. Takaichi, K. Ueda, H. Yagi, T. Yanagitani, and A.A. Kaminskii, Electron. Lett. **42**, 1154 (2006).
[26] J. Dong, A. Shirakawa, K. Ueda, H. Yagi, T. Yanagitani, and A.A. Kaminskii, Appl. Phys. Lett. **90**, 131105 (2007).
[27] J. Dong, A. Shirakawa, K. Ueda, H. Yagi, T. Yanagitani, and A.A. Kaminskii, Appl. Phys. Lett. **90**, 191106 (2007).
[28] E.C. Honea, R.J. Beach, S.C. Mitchell, J.A. Skidmore, M.A. Emanuel, S.B. Sutton, S.A. Payne, P.V. Avizonis, R.S. Monroe, and D.G. Harris, Opt. Lett. **25**, 805 (2000).
[29] T.S. Rutherford, W.M. Tulloch, E.K. Gustafson, and R.L. Byer, IEEE J. Quantum Electron. **36**, 205 (2000).
[30] A. Giesen, H. Hügel, A. Voss, K. Wittig, U. Brauch, and H. Opower, Appl. Phys. B **58**, 365 (1994).
[31] C. Stewen, K. Contag, M. Larionov, A. Giesen, and H. Hugel, IEEE J. Sel. Top. Quantum Electron. **6**, 650 (2000).
[32] J. Dong and K. Ueda, Laser Phys. Lett. **2**, 429 (2005).
[33] H. Yin, P. Deng, and F. Gan, J. Appl. Phys. **83**, 3825 (1998).
[34] P. Yang, P. Deng, and Z. Yin, J. Lumin. **97**, 51 (2002).
[35] H. Qiu, P. Yang, J. Dong, P. Deng, J. Xu, and W. Chen, Mater. Lett. **55**, 1 (2002).
[36] J. Dong, A. Shirakawa, K. Ueda, and A.A. Kaminskii, Appl. Phys. B **89**, 359 (2007).
[37] D.S. Sumida and T.Y. Fan, Opt. Lett. **19**, 1343 (1994).
[38] M. Ito, C. Goutaudier, Y. Guyot, K. Lebbou, T. Fukuda, and G. Boulon, J. Phys.: Condens. Matter **16**, 1501 (2004).
[39] J. Dong, A. Shirakawa, K. Ueda, H. Yagi, T. Yanagitani, and A.A. Kaminskii, Opt. Lett. **32**, 1890 (2007).
[40] X. Xu, Z. Zhao, P. Song, B. Jiang, G. Zhou, J. Xu, P. Deng, G. Bourdet, J.C. Chanteloup, J.-P. Zou, and A. Fulop, Physica B **357**, 365 (2005).
[41] J. Dong, M. Bass, Y. Mao, P. Deng, and F. Gan, J. Opt. Soc. Am. B **20**, 1975 (2003).
[42] X. Xu, Z. Zhao, G. Zhao, P.X. Song, J. Xu, and P. Deng, J. Cryst. Growth **257**, 297 (2003).
[43] Yu.N. Barabanenkov, S.N. Ivanov, A.V. Taranov, E.N. Khazanov, H. Yagi, T. Yanagitani, K. Takaichi, J. Lu, J.F. Bisson, A. Shirakawa, K. Ueda, and A.A. Kaminskii, JETP Lett. **79**, 342 (2004).
[44] J.-F. Bisson, H. Yagi, T. Yanagitani, A. Kaminskii, Yu.N. Barabanenkov, and K. Ueda, Opt. Rev. **14**, 1 (2007).
[45] W. Koechner, Solid State Laser Engineering, Springer Series in Optical Sciences, 5th ed. (Springer-Verlag, Berlin, 1999), p. 236.
[46] J. Kong, D.Y. Tang, J. Lu, and K. Ueda, Opt. Lett. **29**, 65 (2004).